

Synthesis of diamond fine particles on levitated seed particles in an rf CH₄/H₂ plasma chamber equipped with a hot filament

S. Shimizu,¹ T. Shimizu,¹ H. M. Thomas,¹ G. Matern,² R. W. Stark,³ M. Balden,² S. Lindig,² Y. Watanabe,⁴ W. Jacob,² N. Sato,⁵ and G. E. Morfill¹

¹ Max-Planck-Institut für extraterrestrische Physik, Gießenbachstraße, D-85748 Garching, Germany

² Max-Planck-Institut für Plasmaphysik, EURATOM Association, Boltzmannstraße 2, D-85748 Garching, Germany

³ Ludwigs-Maximilians-Universität, Department für Geo- und Umweltwissenschaften, Theresienstraße 41, 80333 München, Germany

⁴ Professor Emeritus, Tohoku University, 6-6 Aoba Aramaki Aoba-ku, Sendai 980-8579, Japan

⁵ Professor Emeritus, Kyusyu University, 744 Motoooka Nishi-ku, Fukuoka 819-0395, Japan

Abstract

The first successful growth of diamond layers on levitated seed particles in CH₄/H₂ plasma is presented. The particles were grown in an rf CH₄/H₂ plasma chamber equipped with a tungsten hot filament. The seed diamond particles injected in a plasma are negatively charged and levitated under the balance of several forces, and diamond chemical vapor deposition takes place on them. The SEM images show that the crystalline structures are formed after the coagulation of islands. The micro-Raman spectroscopy of the particle grown after several hours show the clear peak assigned to diamond.

Published in: Journal of Applied Physics **112**, 073303 (2012); doi: /10.1063/1.4755803

1. Introduction

Fine particles in the size of micro and nanometers are of great interests in many fields, e.g., thin film solar cells,^{1, 2} quantum effect devices,^{3, 4} catalysis,⁵ medicine,⁶ electrodes for fuel cells,⁷ etc. Those particles are designed to exhibit useful functions with relation to the material properties determined by fabrication methods and adopted conditions. Among many production methods, plasma enhanced chemical vapor deposition (PECVD) is one of the useful techniques from the viewpoint of controllability of growth at atomic levels. Boufendi et al. showed the growth of crystalline silicon fine particles with pulsed plasmas,³ and Hayashi et al. observed the growth of amorphous carbon layers on levitated seed amorphous carbon particles in rf CH₄/H₂ plasmas.⁸ In our previous study, we succeeded in levitating diamond seed particles in an rf CH₄/H₂ plasma at the temperature of 1300 K for more than 10 h, and the island growth of diamond was observed on them.⁹ To enhance the growth further more, in this study, the deposition setup was upgraded with a hot filament. Note that, rf plasma is also necessary to levitate particles, allowing homogeneous growth on the whole particle surface. Therefore, the hot filament was equipped in an rf plasma system. In general, the optimum substrate temperature for CVD diamond growth is in the range of 1200–1300 K.¹⁰ First of all, the hot filament provides effective heating of the particles due to heat radiation, contributing crystalline diamond growth. Second, it generates a higher density of atomic hydrogen from the H₂ gas than a low temperature rf plasma alone.^{11, 12} A high atomic hydrogen density is one of the essential factors for crystalline diamond growth:¹³⁻¹⁵ 1) atomic hydrogen react with carbon sp² bonds and reduce their amount, 2) it lowers the surface energy of growing diamond by terminating a surface dangling bond, preventing graphic-like surface reconstructions.^{14, 16} Additionally, it has been indicated that the nanoparticles in a gas phase can be locally heated by the energy damping through the attachment of atomic hydrogen to a growing surface, resulting in crystalline formation.^{17, 18} In this study, diamond layers were grown on the levitated seed particles using the above system, and their morphologies and structures were analyzed.

2. Experiment

The details of the growth chamber used in this study are described elsewhere.¹⁹ The bottom electrode is driven by rf voltage and the top electrode is grounded. A hot filament is equipped between the two electrodes. On the bottom electrode, a particle confinement ceramic ring is placed to modify sheath electric field so that the particles are confined above the inside region of the ring. The seed diamond particles (size = 2–4 μm , Nilaco) are stored in the dispenser, and their surfaces are not pre-treated. Prior to the growth experiment, the filament was baked and carburized. The baking conditions are: H_2 flow = 100 sccm, pressure = 330 Pa, filament temperature = 1500 K, baking time = 30 min. The carburization conditions are: CH_4 flow = 2 sccm, H_2 flow = 200 sccm, pressure = 330 Pa, filament temperature = 2400 K, carburization time = 2 h. Without this filament pre-treatment, tungsten deposition occurs on the growing particles as detected by Energy Dispersive X-ray (EDX). After deposition, the levitated particles are captured directly on a Si substrate applying a method described elsewhere.¹⁹ The surface morphologies of the particles are imaged by scanning electron microscope (SEM), (Helios NanoLab 600, FEI), and their bond configurations are investigated by confocal micro-Raman spectroscopy (CRM 200, WITec, excitation wavelength: 532 nm). Peak position of the Raman system is calibrated with a crystalline diamond substrate prior to the measurements.

3. Results and discussion

Fig. 1 shows an image of the levitated particles in the rf CH_4/H_2 plasma with the hot filament in operation. The hot filament is not visible in the image. It is located ca. 5 cm above the upper edge of the ceramic ring and therefore above the upper edge of the image. Fine particles with diameters of a few micrometers or less are negatively charged and levitated in the plasma sheath due to a balance of several forces, including gravity, electrostatic, thermophoretic, ion drag and others.²⁰ Since they are all negatively charged, there are repulsive forces between the particles so that growth can take place on individual seed particles. The applied conditions are: CH_4 = 2 sccm, H_2 = 200 sccm, pressure = 330 Pa, filament temperature = 2400 K, rf input power = 50 W bottom electrode temperature = 1300 K, top electrode temperature = 900 K. Several steps are required to achieve steady

state conditions for diamond growth on levitated particles. First, H_2 rf plasma is ignited at 300 K; then the seed particles are inserted and levitated in the plasma. The total pressure during this initial phase is set to 130 Pa. After confirming the levitation, temperatures of the electrodes and the filament are increased. This increase must be gradual so that levitation is not significantly disturbed.²¹ During this phase also the total pressure is increased from 130 to 330 Pa. Higher pressure gives thinner plasma sheath thickness in our parameter range, resulting in lowering the particle levitation position. The force balance on the levitated particles is determined also by temperature and rf input power. In this phase, due to the high bottom electrode temperature, the particles are levitated at a higher position than that observed at 130 Pa and 300 K mostly due to the additional thermophoretic force. It takes about 30 minutes until the temperatures reach steady state condition, and during this phase the surfaces of the particles are exposed to pure H_2 plasma. After steady state conditions are established, CH_4 gas is admixed to start growth. Particles are levitated in stable positions throughout the complete growth process.

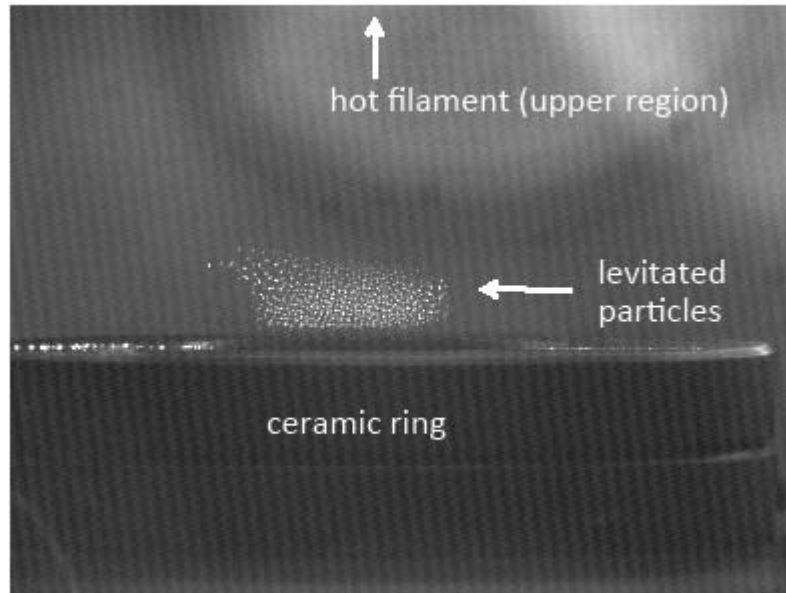


FIG. 1: Levitated diamond particles in the rf CH_4/H_2 plasma with a hot filament. The conditions are: filament temperature = 2400 K, bottom electrode temperature = 1360 K, top electrode temperature = 800 K, total pressure = 330 Pa, rf input power 50 W, CH_4 = 2 sccm, H_2 = 200 sccm.

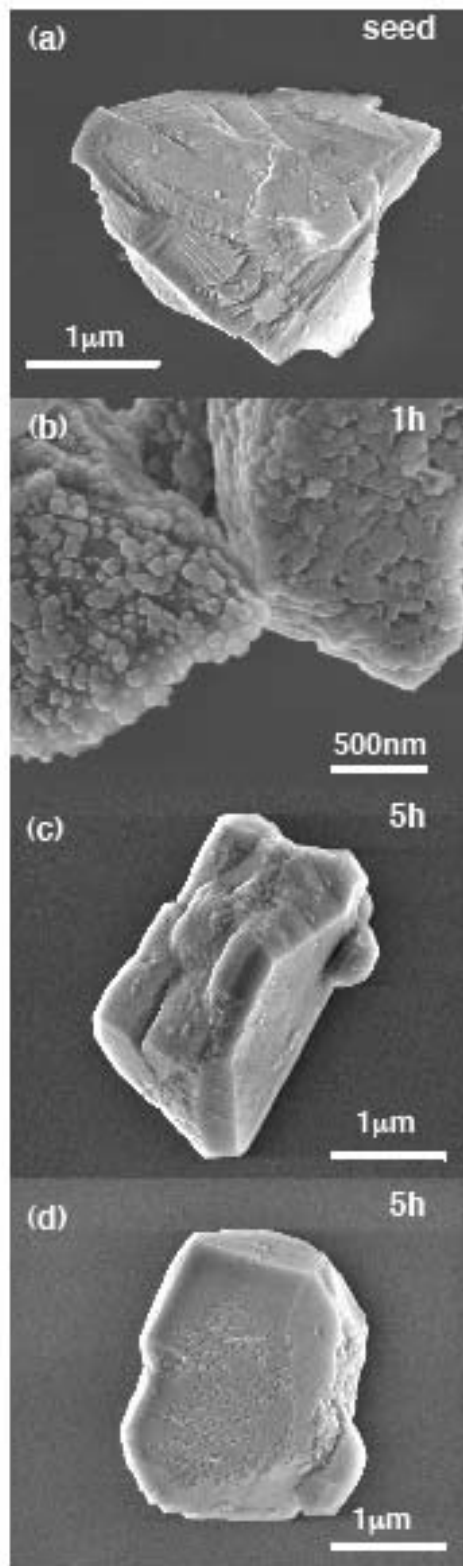


FIG. 2.
SEM images of the grown particles: (a) seed particle without growth, (b) after 1 h growth, (c), (d) after 5 h growth.

Fig. 2 (a) shows the morphology of a seed particle prior to deposition. Figs. 2 (b)–(d) are SEM images of particles exposure to growth conditions for different times. After 1 h growth, small grains are visible on the surfaces of the seed particles as shown in Fig. 2 (b). It is also observed that some of the islands start coagulating. The size of the grains before coagulation is roughly 100 nm. Figs. 2 (c) and (d) are the images of two different particles grown after 5 h where flat surfaces and edge-like structures are observed, indicating crystalline growth. It seems that the growth is in a Volmer-Weber (VM) mode, which is generally observed in heteroepitaxial growth. In an X-ray photo-electron spectroscopy (XPS) measurement, an oxygen peak is detected on the surface of the initial seed particles. Those oxygen surface layers could inhibit homoepitaxial growth in a Frank-van der Merwe (FM) mode. On the other hand, the surface oxygen atoms are thermally desorbed above 1200 K,²² or it could be replaced with hydrogen atoms by atomic hydrogen exposure,²² which is the procedure used in our study before the diamond layer growth as described above. Additionally, the effect of a substrate temperature should also be considered. Kamo et al. has reported the polycrystalline diamond growth on a diamond substrate at a low substrate temperature.²³ At low temperatures, the surface of a diamond substrate, a seed particle in our case, are most likely terminated with oxygen or hydrogen atoms because no thermal desorption of them take place.^{15, 22} Note that, the substrate temperature of around 1300 K, which is commonly accepted as the optimum value for high quality homoepitaxial diamond growth, is also the temperature at which thermal desorption of hydrogen and, as a result, surface reconstructions of diamond take place.^{15, 16} Those simultaneous procedures are believed to be related to high quality homoepitaxial diamond growth. At low temperatures, since the growing surface is terminated with H or O atoms, the sticking sites for diamond growth, i.e. surface dangling bonds, should be created through chemical reactions, e.g., with atomic hydrogen or other hydrocarbon radicals in a gas phase, and it has been shown that it requires far less activation energy than that for a spontaneous desorption of hydrogen from a diamond (100) surface.²⁴ In such a case, the density of surface dangling bonds at a steady state condition is influenced by the flux of atomic hydrogen or other radicals. Note that, a created dangling bond can also be terminated with another atomic hydrogen. If the number of the sticking sites is limited, it can be a cause of island growth of diamond at low temperatures because of different surface energies between diamond and such hydrogen or oxygen terminated surface.^{14, 25, 26} In our case, although the bottom electrode temperature was fixed at 1300 K and the levitated particles

were additionally heated with the hot filament, the temperature of those particles could be still lower than the optimum value. In the high substrate temperature case (> 1400 K), generally non-diamond components are grown,¹⁴ which is, at least, not our case as confirmed by the Raman measurement. To understand the growth mode furthermore, the growing surface structure should be checked as a function of growth temperature. Additionally, the surface analysis of the seed particles exposed to atomic hydrogen, and the temperature measurement of the levitated particles could also help to understand the growth mode.

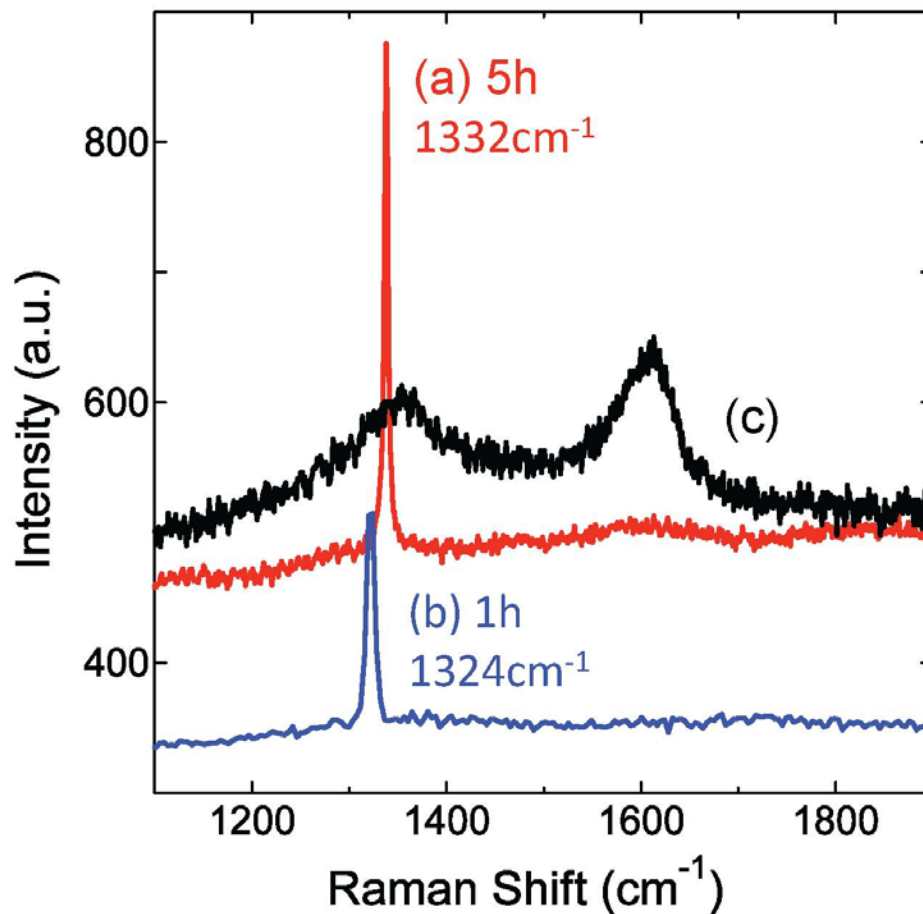


FIG. 3.

Micro-Raman spectrum of the grown particles at various conditions. (a) particles grown at the filament temperature of 2400 K for 5 h, (b) particles grown at the filament temperature of 2400 K for 1 h, (c) particles grown at the filament temperature of 1800 K for 5h.

The grown particles were investigated by micro-Raman spectroscopy. Fig. 3 shows the result. Spectrum (a) is taken from one of the particles grown for 5 h. One can see the sharp peak assigned to diamond at 1332 cm^{-1} , indicating crystalline diamond growth. Spectrum (b) is taken from a particle grown for 1 h, and the peak assigned to diamond is also observed. In this case, the observed peak position is shifted from 1332 cm^{-1} to 1324 cm^{-1} . The similar trend was observed in our former work.²¹ Such peak shift is generally observed when a crystalline size is small, which is explained by residual stress,²⁷⁻³¹ or by phonon confinement effect in each crystal grains.^{32, 33} The correlation between the peak shifts and defect densities has also been reported, suggesting the influence of grain boundaries, therefore, the size and density of grains.³⁴ Additionally, the peak shifts were observed due to the heating up of a measurement target by probing laser.^{13, 35, 36} In our case, the typical sizes of the crystal grains are larger than 100 nm (see Fig. 2 (b)) which seems to be rather large to discuss the internal stress causing the observed relatively large peak shifts of around 10 cm^{-1} . Such amount of shift is also observed in hexagonal diamond with peak broadening.^{37, 38} At the earlier stage of the growth in our case, such hexagonal diamonds might be grown. On the other hand, the peak shift is not observed in the diamond layers grown after 5 h. More detailed analysis, e.g. XRD measurement to identify lattice structures,³⁹ grain size and laser intensity dependent Raman measurements and electron paramagnetic resonance (EPR) measurement to analyze defect densities should help to understand the origins of the peak shift observed in our study.

Since the diamond layers are grown on a seed diamond particle, it is important to confirm that the detected signal is not from the seed particle but from the grown layers. First of all, the micro-Raman spectroscopy used in this study is a confocal system having the depth resolution of about $1\text{ }\mu\text{m}$. Second, when graphite or amorphous carbon layers are grown on the surfaces, e.g. by changing the filament temperature, only the typical D-peak (1353 cm^{-1}) and the G-peak (1610 cm^{-1}) are observed, but no diamond signal from the inner seed is detected. Spectrum (c) in Fig. 3 shows the Raman signal of the particle grown at the filament temperature of 1800 K. Obviously, at the low filament temperature, no diamond layers are grown. A lower filament temperature causes a lower dissociation of the H_2 gas and possibly leads to a lower temperature of the levitated particles. Both can be the reason that no diamond layers are grown.^{10, 14, 15} The absorption coefficient (α) of amorphous carbon changes due to its structure. The α value of the amorphous carbon prepared or annealed at the temperature of around several hundred K is of the order of 10^5 cm^{-1} at

530 nm,^{40, 41} which gives the penetration depth of 100 nm, and that of graphite is 3×10^5 cm⁻¹ at 539 nm,⁴² giving the penetration depth of 30 nm. Additionally, Raman efficiency of graphite is two orders of magnitude higher than that of diamond.⁴³ Therefore, even a very slight amount of graphite is detectable with Raman spectroscopy. On the other hand, the spectrum (a) and (b) in Fig. 3 only show the diamond peaks, indicating that those are the signals from the grown layers, or it is at least the sum of the signals from the grown layers and the seed particles.

4. Conclusion

First successful growth of diamond layers on levitated seed diamond particles in the rf plasma chamber equipped with a hot filament is demonstrated. The SEM images show that the crystalline structures are formed after the coagulation of islands. The micro-Raman spectroscopy of the grown particle show the clear peak assigned to diamond.

Acknowledgements

The authors would like to acknowledge C. Linsmeier in Max-Planck-Institut für Plasmaphysik, EURATOM Association in Germany for the XPS measurement and discussion, and one of the authors (S. S.) would like to acknowledge A. Matsuda in Osaka University in Japan for useful discussions.

References

- ¹ M. Ito, S. Shimizu, M. Kondo, and A. Matsuda, *J. Non-Cryst. Solids* **338–340**, 698 (2004).
- ² M. Green, *Third generation photovoltaics*, (Springer-Verlag, Berlin, Heidelberg, 2003).
- ³ A. Bouchoule, and L. Boufendi, *Plasma Sources Sci. Technol.* **2**, 204 (1993).
- ⁴ T. Kamiya, K. Nakahata, Y. T. Tan, Z. A. K. Durrani, and I. Shimizu, *J. Appl. Phys.* **89**, 6265 (2001).
- ⁵ M. Date, M. Okumura, S. Tsubota, and M. Haruta, *Angew. Chem. Int. Ed.*, **43**, 2129 (2004).
- ⁶ T. Nakagawa, S. Kondo, Y. Sasai, and M. Kuzuya, *Chem. Pharm. Bull.* **54**, 514 (2006).
- ⁷ H. Liu, C. Songa, L. Zhang, J. Zhang, H. Wang, and D. P. Wilkinson, *J. Power Sources* **155**, 95 (2006).
- ⁸ Y. Hayashi and K. Takahashi, *Jpn. J. Appl. Phys.* **36**, 4976 (1997).
- ⁹ T. Shimizu, W. Jacob, H. Thomas, G. Morfill, T. Abe, Y. Watanabe, and N. Sato, *Thin Solid Films* **506-507**, 652 (2006).
- ¹⁰ E. Kondoh, T. Ohta, T. Mitomo, and K. Ohtsuka, *J. Appl. Phys.* **72**, 705 (1992).
- ¹¹ H. Umemoto K. Ohara D. Morita, Y. Nozaki, A. Masuda, and H. Matsumura, *J. Appl. Phys.* **91**, 1650 (2002).
- ¹² L. L. Connell, J. W. Fleming, H. N. Chu, D. J. Vestyck jr., E. Jensen, and J. E. Butler, *J. Appl. Phys.* **78**, 3622 (1995).
- ¹³ S. S. Lee, D. W. Minsek, D. J. Vestyck, and P. Chen, *Science* **263**, 1596 (1994).
- ¹⁴ H. Liu, and D. S. Dandy, *Diamond chemical vapor deposition*, (Noyes publications, New Jersey 1995) p. 42, 80, 147.
- ¹⁵ A. R. Badzian, and R. C. DeVries, *Mater. Res. Soc. Bull.* **23**, 385 (1988).
- ¹⁶ B. B. Pate, *Surf. Sci.* **165**, 83 (1986).
- ¹⁷ H. Vach, and Q. Brulin, *Phys. Rev. Lett.* **95**, 165502 (2005).
- ¹⁸ A. Sutoh, Y. Okada, S. Ohta, and M. Kawabe, *Jpn. J. Appl. Phys.* **34**, L1379 (1995).
- ¹⁹ S. Shimizu, T. Shimizu, W. Jacob, H. M. Thomas, and G. E. Morfill, *Phys. Plasma* **18**, 113703 (2011).
- ²⁰ V. E. Fortov, A. G. Khrapak, S. A. Khrapak, V. I. Molotkov, and O. F. Petrov, *Physics – Uspekhi* **47**, 447 (2004).
- ²¹ S. Shimizu, T. Shimizu, B. M. Annaratone, W. Jacob, C. Linsmeier, S. Lindig, R. W. Stark, F. Jamitzky, H. Thomas, N. Sato, and G. E. Morfill, *Appl. Surf. Science* **254**, 177 (2007).
- ²² M. Z. Hossain, T. Kubo, T. Aruga, N. Takagi, T. Tsuno, N. Fujimori, M. Nishijima, *Surf. Science* **436**, 63 (1999).

- ²³ M. Kamo, H. Yurimoto, and Y. Sato, *Appl. Surf. Sci.* **33–34**, 553 (1988).
- ²⁴ C. Kanai, K. Watanabe, Y. Takakuwa, *Appl. Surf. Sci.* **159–160**, 599 (2000).
- ²⁵ X. Jiang, C. P. Klages, R. Zachai, M. Hartweg, and H. J. Fusser, *Appl. Phys. Lett.* **62**, 3438 (1993).
- ²⁶ Y. Kaibara, K. Sugata, M. Tachiki, H. Umezawa, and H. Kawarada, *Diamond Relat. Mater.* **12**, 560 (2003).
- ²⁷ M. H. Grimsditch, E. Anastassakis, and M. Cardona, *Phys. Rev.* **B 18**, 901 (1978).
- ²⁸ H. Boppart, J. van Straaten, and I. F. Silvera, *Phys. Rev.* **B 32**, 1423 (1985).
- ²⁹ J. Michler, M. Mermoux, Y. von Kaenel, A. Haouni, G. Lucazeau, and E. Blank, *Thin Solid Films* **357**, 189 (1999).
- ³⁰ J. Zi, H. Büscher, C. Falter, W. Ludwig, K. Zhang, and X. Xie, *Appl. Phys. Lett.* **69**, 200 (1996).
- ³¹ M. Yoshikawa, Y. Mori, M. Maegawa, G. Katagiri, H. Ishida, and A. Ishitani, *Appl. Phys. Lett.* **62**, 3114 (1993).
- ³² J. W. Ager III, D. K. Veirs, and G. M. Rosenblatt, *Phys. Rev.* **B 43**, 6491 (1991).
- ³³ Y. Namba, and E. Heidarpour, *J. Appl. Phys.* **72**, 1748 (1992).
- ³⁴ T. A. Nachal'naya, V. D. Andreyev, and E. V. Gabrusenok, *Diamond Relat. Mater.* **3**, 1325 (1994).
- ³⁵ G. Viera, S. Huet, E. Bertran, and L. Boufendi, *J. Appl. Phys.* **90**, 4272 (2001).
- ³⁶ X. Zhao, K. A. Cherian, R. Roy, and W. B. White, *J. Mater. Res.* **13**, 1974 (1998).
- ³⁷ D. S. Knight, and W. B. White, *J. Mater. Res.* **4**, 385 (1989).
- ³⁸ H. He, T. Sekine, and T. Kobayashi, *Appl. Phys. Lett.* **81**, 610 (2002).
- ³⁹ S. R. P. Silva, G. A. J. Amaratunga, E. K. H. Salje, and K. M. Knowles, *J. Mater. Sci.* **29**, 4962 (1994).
- ⁴⁰ F. W. Smith, *J. Appl. Phys.* **55**, 764 (1984).
- ⁴¹ E. Pascual, C. Serra, and E. Bertran, *J. Appl. Phys.* **70**, 5119 (1991).
- ⁴² E. D. Palik, *Handbook of Optical Constants of Solids II*, (Academic Press Inc, San-Diego, 1991) p. 449.
- ⁴³ N. Wada, and S. A. Solin, *Physica* **105B**, 353 (1981).